



## Open Archive Toulouse Archive Ouverte (OATAO)

OATAO is an open access repository that collects the work of Toulouse researchers and makes it freely available over the web where possible.

This is an author-deposited version published in: <http://oatao.univ-toulouse.fr/>  
Eprints ID : 2879

**To link to this article :**

URL : <http://dx.doi.org/10.1149/1.3039090>

**To cite this version :** Recham , N. and Armand, M. and Laffont-Dantras, Lydia and Tarascon, Jean-Marie ( 2009) [\*Eco-Efficient Synthesis of LiFePO4 with Different Morphologies for Li-Ion Batteries.\*](#) Electrochemical and Solid State Letters, vol. 12 (n° 2). A39-A44. ISSN 1099-0062

Any correspondence concerning this service should be sent to the repository administrator: [staff-oatao@inp-toulouse.fr](mailto:staff-oatao@inp-toulouse.fr)

# Eco-Efficient Synthesis of LiFePO<sub>4</sub> with Different Morphologies for Li-Ion Batteries

N. Recham, M. Armand, L. Laffont, and J-M. Tarascon<sup>z</sup>

Laboratoire de Réactivité et Chimie des Solides, Université de Picardie Jules Verne, CNRS UMR6007, 80039 Amiens, France

LiFePO<sub>4</sub> is presently the most studied electrode material for battery applications. It can be prepared via solution, although it requires well-controlled pH conditions to master the iron valence state in the newly created material. Here we report its synthesis via the use of “latent bases” capable of releasing a nitrogen base upon heating. This way of controlling the reaction pH enables, in the absence of excess Li, the preparation of Fe<sup>+3</sup>-free LiFePO<sub>4</sub> powders having various morphologies and showing good electrochemical performance. This approach is shown to offer great opportunities for the low-temperature synthesis of various electrode materials.

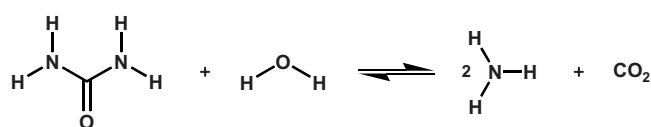
DOI: 10.1149/1.3039090

Rechargeable Li-ion cells, which are powering most of today’s portable electronics, are strongly considered for automotive transportation. Yet, safety and cost issues remain to be solved, prior to seeing this environmentally much-needed market extend globally.<sup>1</sup> The cost is mainly determined by the material abundance, thus 3d metal redox elements, such as in LiFePO<sub>4</sub>,<sup>2</sup> are receiving increased attention, while Co- or Ni-based electrodes are electronic market niches. The carbon nanopainting techniques, applied to insulating LiFePO<sub>4</sub>, yield high-rate yet safe batteries.<sup>3</sup> The environmental attractiveness of LiFePO<sub>4</sub> prevails over an energy density penalty due to low packing density, even more so in the presence of carbon. LiFePO<sub>4</sub> is the main contender for electric vehicle automakers, but natural sources of triphylite are scarce. Synthetic triphylite has to be made with directly processable grain sizes while looking for the most expeditious and energy-saving carbon coating.

Precipitation from aqueous medium, under normal pressure<sup>4</sup> or in autoclave,<sup>5,6</sup> is often preferred to ceramic methods; the latter require high temperatures to ensure the diffusion of the reactants and the growth of the grains; they therefore demand high energy while leading to highly polydispersed powders. Precipitation methods in liquid media (e.g., solvothermal synthesis)<sup>7</sup> require little energy, and if nucleation and growth phenomena are controlled, the size distribution is much narrower.

Basically, a solvothermal synthesis reaction consists in reacting metal/nonmetal-based soluble salts with a base, and increasing the temperature to promote the growth of the desired phase via Ostwald ripening. Inherent drawbacks are formation of hydroxides from the metals used, without any control over the nucleation step and possible oxidation by air oxygen. This is particularly worrisome in the case of Fe<sup>II</sup> and cobalt<sup>II</sup>.

Hydrothermal synthesis of lithium iron phosphate, according to the reaction  $\text{H}_3\text{PO}_4 + \text{FeSO}_4 + 3\text{LiOH} \Rightarrow \text{LiFePO}_4 + \text{Li}_2\text{SO}_4 + 3\text{H}_2\text{O}$ , has been demonstrated,<sup>8</sup> though some Fe<sup>(III)</sup> impurities remain in the final product. More recently, Delacourt et al.<sup>4</sup> succeeded in preparing at low temperature (ca. 108°C) electrochemically active LiFePO<sub>4</sub> nanoparticles having a few percent of Fe<sup>+3</sup>.<sup>9,10</sup> via a precipitation process in a pH range close to neutrality using a water-dimethyl sulfoxide acidic mixture containing equimolar amounts of 0.1 M FeSO<sub>4</sub>·7H<sub>2</sub>O and H<sub>3</sub>PO<sub>4</sub>, to which they added dropwise 0.3 M LiOH solution (e.g., to end with a Li/Fe/P molar ratio of 3:1:1). For either hydrothermal or precipitation processes, there are drawbacks (i) the use of costly LiOH in threefold excess (compared to LiFePO<sub>4</sub>) and then the need to recycle Li<sub>2</sub>SO<sub>4</sub>, falling short of the economy of atoms now sought in industrial chemistry, and (ii) the increased risk of forming Fe(OH)<sub>2</sub> precursor to Fe<sup>+3</sup> impurities in the final product, respectively. Ferric species are thought to be responsible for the leaching of metal ions in the electrolyte and



Scheme 1.

through their reduction products, increasing the impedance of the anode.<sup>11</sup> All of these aforementioned issues are detrimental to reproducible and low-cost manufacturing.

To remedy these issues, we searched for different synthetic approaches and have been inspired by recent studies aiming toward the low-temperature synthesis of various inorganic compounds, either in bulk or nanocrystalline forms, such as ammonium–thorium phosphates,<sup>12</sup> cerium biphosphate, hydrotalcites,<sup>13</sup> TiO<sub>2</sub>,<sup>14</sup> La<sub>0.8</sub>Sr<sub>0.2</sub>Ga<sub>0.8</sub>Mg<sub>0.2</sub>O<sub>2.8</sub>,<sup>15</sup> or (NH<sub>4</sub>)<sub>2</sub>Ce(PO<sub>4</sub>)<sub>2</sub>·H<sub>2</sub>O,<sup>16</sup> via the use of a basic medium created by the temperature-driven decomposition of urea. Herein we implemented the aforementioned approach to the synthesis of tailor-made LiFePO<sub>4</sub> powders via a solvothermal process in either aqueous or nonaqueous solvents. This synthesis does not rely on the use of LiOH but rather on the use of additives (urea, hexamethylene tetramine, and others), which upon mild heating liberate in situ the basic species needed to complete the precipitation reaction.

The use of urea as an initially neutral chemical yielding NH<sub>3</sub> and CO<sub>2</sub> upon hydrolysis at 90°C according to Scheme 1 has been suggested as early as 1989 by Matijevic’s group<sup>17–19</sup> for the precipitation of alkaline earth carbonates, but in this case, CO<sub>2</sub> is immediately trapped as CO<sub>3</sub><sup>2-</sup> in the lattice, displacing the equilibrium. However, the preparation of the olivines using latent bases is not known and an essential difference is the need to go > 100°C, below which the anhydrous LiFePO<sub>4</sub> does not form.

In light of this previous work on forced hydrolysis, we first attempted the hydrothermal synthesis of LiFePO<sub>4</sub> in aqueous medium as follows. Urea and LiH<sub>2</sub>PO<sub>4</sub> in a molar ratio 1.2:1, so as to have a slight excess of NH<sub>3</sub> to neutralize LiH<sub>2</sub>PO<sub>4</sub> and raise the solution pH through the reaction, were dissolved under magnetic stirring in water during 10 min. Stoichiometric (Li/P = 1:1) amount of FeSO<sub>4</sub>·7H<sub>2</sub>O to produce LiFePO<sub>4</sub> is then added to the solution. After 5 min of magnetic stirring, the solution, which pH is 3.4, is poured into a poly(tetrafluoroethylene) (PTFE) container which is placed in an autoclave. Once the atmosphere of the autoclave has been deoxygenated by flushing with argon, the solution temperature, while being maintained under constant agitation, was increased to 180°C at a rate of 1°C/min, maintained at that temperature for 3 h, then left to cool to ambient temperature. The recovered greenish suspension was then filtered, washed, and dried (Fig. 1). The X-ray diffraction (XRD) pattern, recorded on a Bruker D8 Advance diffractometer (Cu Kα radiation, λ<sub>1</sub> = 1.54053 Å) indicates the pres-

<sup>z</sup> E-mail: jean-marie.tarascon@sc.u-picardie.fr

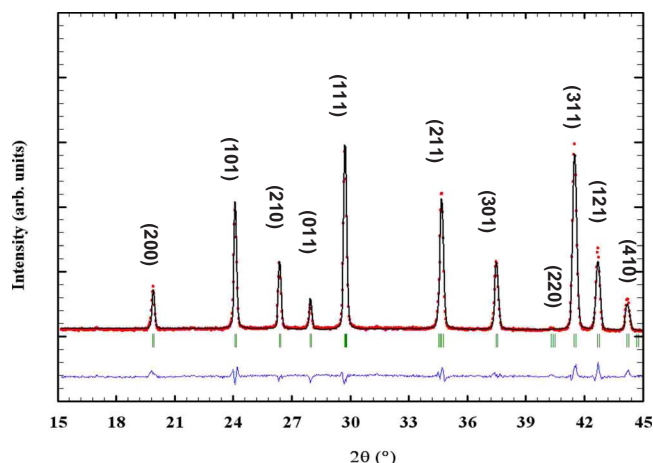


**Figure 1.** (Color online) Rietveld refinement for  $\text{LiFePO}_4$  made in water. Experimental X-ray powder diffraction pattern (dotted curve) compared to the Rietveld-refined profile (continuous line) and difference curve.

ence of the single-phase  $\text{LiFePO}_4$ , as all the peaks were entirely indexed in the space group  $Pnma$ . The lattice parameters  $a = 10.3601 \text{ \AA}$ ,  $b = 6.0027 \text{ \AA}$ ,  $c = 4.7075 \text{ \AA}$ ;  $V = 292.75 \text{ \AA}^3$ , obtained from full pattern matching refinements via the program Fullprof<sup>20</sup> using the pseudo-Voigt profile function of Thompson et al.,<sup>21</sup> are in good agreement with literature reports.<sup>22-24</sup>

To gain insight into the reacting path leading to the growth of  $\text{LiFePO}_4$ , we monitored the variation of the pH together with the nature of the phases formed as a function of time for various temperatures. To do so, the autoclave was equipped with an in situ sampling device, allowing intermittent aliquots to withdraw while the reaction proceeded. In a typical experiment the reaction mixture was placed in the autoclave and flushed with  $\text{N}_2$  gas prior to turning on the autoclave mantle heater. A ramp of  $1^\circ\text{C}/\text{min}$  was used to reach 150 and  $180^\circ\text{C}$  (pressures  $\approx 10$  and  $20$  bars, respectively). Once such isothermal temperatures were reached (time  $T_0$ ), samples were intermittently withdrawn. The samples were first checked for their pH and the solids twice centrifuged and filtered through a  $0.1 \text{ mm}$  filter (Millipore) and X-rayed. Figure 2a shows the evolution of pH as a function of time, implying the efficient and rapid hydrolysis of the urea additive because at  $180^\circ\text{C}$  the pH of the solution becomes basic in  $\sim 40$  min, while, as expected, it takes  $\sim 60$  min at  $150^\circ\text{C}$ . In parallel, XRD data (Fig. 2b) indicate that under such experimental conditions the growth of  $\text{LiFePO}_4$  enlists sequentially the appearance, at an early stage of the reaction, of  $\text{Fe}_3(\text{PO}_4)_2 \cdot 8\text{H}_2\text{O}$  (vivianite), which after  $\sim 40$  min leads to the dehydrated version  $\text{Fe}_3(\text{PO}_4)_2$ , which transforms into  $\text{LiFePO}_4$  over the next hundred minutes. The same sequence, but with longer time intervals, occurs at lower temperatures. The scanning electron microscopy (SEM) images of the powders, taken with a field emission gun (FEI Quanta F200P), revealed nicely crystallized  $2\text{--}4 \text{ }\mu\text{m}$  cubic particles having salient facets (Fig. 3a), regardless of whether they were prepared at either 150 or  $180^\circ\text{C}$ . Temperatures lower than  $120^\circ\text{C}$  fail in producing  $\text{LiFePO}_4$  powders. Finally, Mössbauer measurements recorded in transmission mode (data not shown) on the micrometric samples repeatedly indicate amounts of  $\text{Fe}^{3+}$  falling within the  $0\text{--}1\%$  range and they are stable in time. Nanometric samples kept in laboratory atmosphere, however, tend to oxidize. The details of such results will be addressed in a forthcoming paper.

Because this approach was validated, it was extended to the use of numerous molecules, some of which were previously used such as amines<sup>25</sup> that could produce in situ, via a solvolysis reaction or via a temperature-controlled decarboxylation, Brønsted or Lewis bases necessary to the formation of  $\text{LiFePO}_4$ . Table I captures some of the molecules (guanidinium or isocyanate salts, hexamethylene-

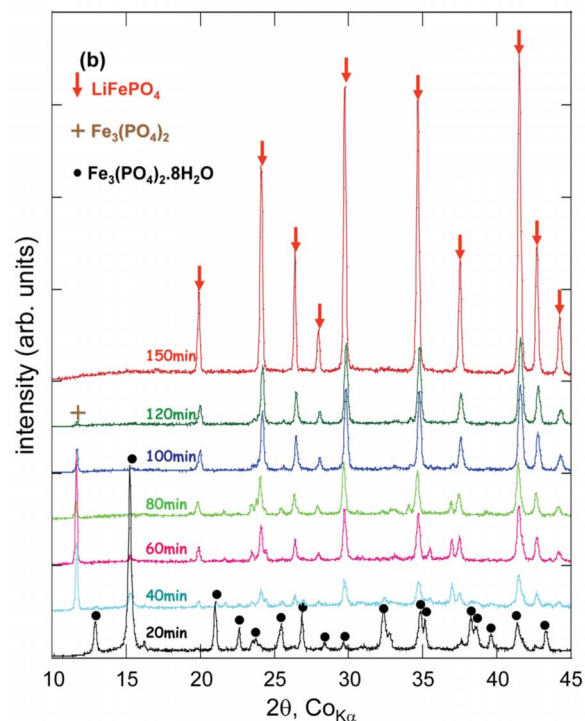
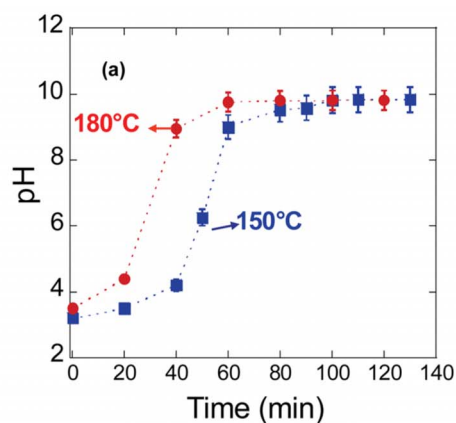


**Figure 2.** (Color online) In situ monitoring of the solvothermal reaction with (a) variation of pH of the solution as a function of time for two distinct experiments run separately at 150 and  $180^\circ\text{C}$  and (b) structural evolution of the precipitated materials for the same samples as in (a).

tetramine), together with their hydrolysis reaction in water at mild temperatures, which we have successfully used. In all cases, yields were 100%, within error for losses during filtration/washing. For conciseness, rather than giving a detailed experimental description of all  $\text{LiFePO}_4$  specimens prepared using various combinations of solvents and latent bases which are summarized in Table II together with the lattice parameters of the obtained phases, we focused on an additional aspect which lies in the nature/choice of a solvolysis agent chemically compatible with the “latent bases” to trigger the liberation of a base.

Water is by all means the most popular solvolysis agent, but other polar liquids containing OH groups such as diols or amides can be used as previously reported,<sup>26</sup> hence providing a myriad of opportunities to adjust the morphology/texture of the newly born phases. 1,2-propanediol (to avoid toxic 1,2-ethanediol) was first tried, as an alternative to water, on the basis of the reaction in Scheme 2, which we have shown to occur at around  $150^\circ\text{C}$ . Such a finding was applied to the hydrothermal synthesis of  $\text{LiFePO}_4$ . Stoichiometric amounts of  $\text{LiH}_2\text{PO}_4$  and urea in slight excess (for rea-

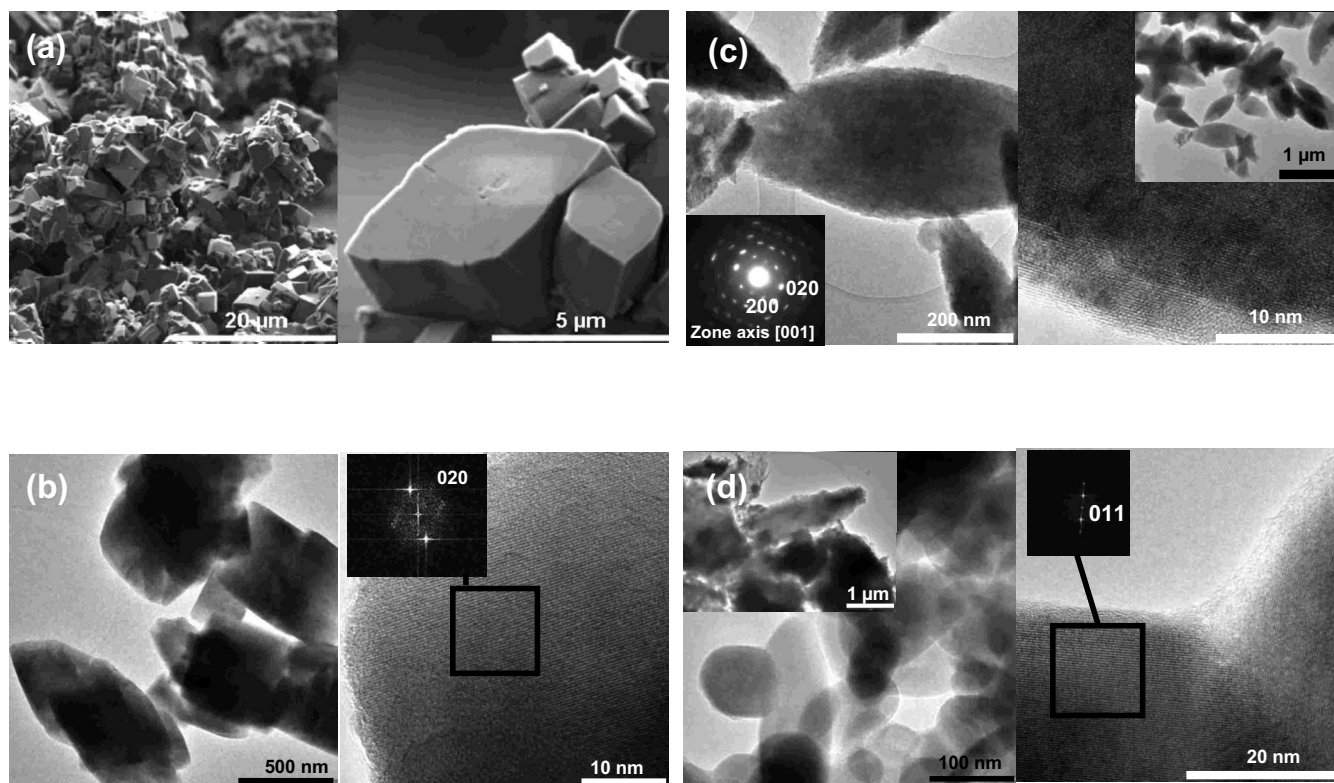


**Figure 3.** SEM images for  $\text{LiFePO}_4$  powders made in water are shown in (a), while the TEM/HRTEM images for powders grown in water/diol, formamide/diol, and DMF-diol are shown in (b), (c), and (d) (inset left: DMF before heating, right after heating at  $680^\circ\text{C}$ ), respectively. For each picture, the bright-field images give information on the particle shape and size (left) combined with a selected area diffraction (SAED) pattern only for (c). HRTEM images and SAED were combined with Fourier transform, providing structural details both at the core and surface material level, with the presence of a well-defined carbon layer covering the particles when DMF was used.

sons already described) were dissolved under magnetic stirring in 1,2-propanediol, to which we added the right amount of  $\text{FeSO}_4 \cdot 7\text{H}_2\text{O}$  to produce  $\text{LiFePO}_4$ . The solution was placed into an autoclave in which the temperature was raised to  $180^\circ\text{C}$  in 2 h and maintained for 24 h, the time that we determined necessary after several trials to obtain a complete reaction; nicely crystallized  $\text{LiFePO}_4$  powders having the following lattice parameters  $a = 10.3470 \text{ \AA}$ ,  $b = 6.0032 \text{ \AA}$ ,  $c = 4.6997 \text{ \AA}$ , and  $V = 291.92 \text{ \AA}^3$  resulted. We found that the particle size and morphology of the powders can be deliberately modified using varying water/1,2-propanediol mixtures, with smaller particle sizes (200 nm), having platelet shapes obtained for an 80:20% water/1,2-propanediol volume ratio as apparent from transmission electron microscopy (TEM) (Fig. 3b) using a FEI Tecnai F20 S-TWIN microscope. The bright-field image (Fig. 3b; left) shows platelet-shaped particles with sizes ranging from 200 to 800 nm. One part of the bright-field image has been studied in high resolution showing that the  $\text{LiFePO}_4$  particles are monoliths. Overall, the powders prepared in diol-based solvents were always found to be more dispersed than those prepared in pure water.

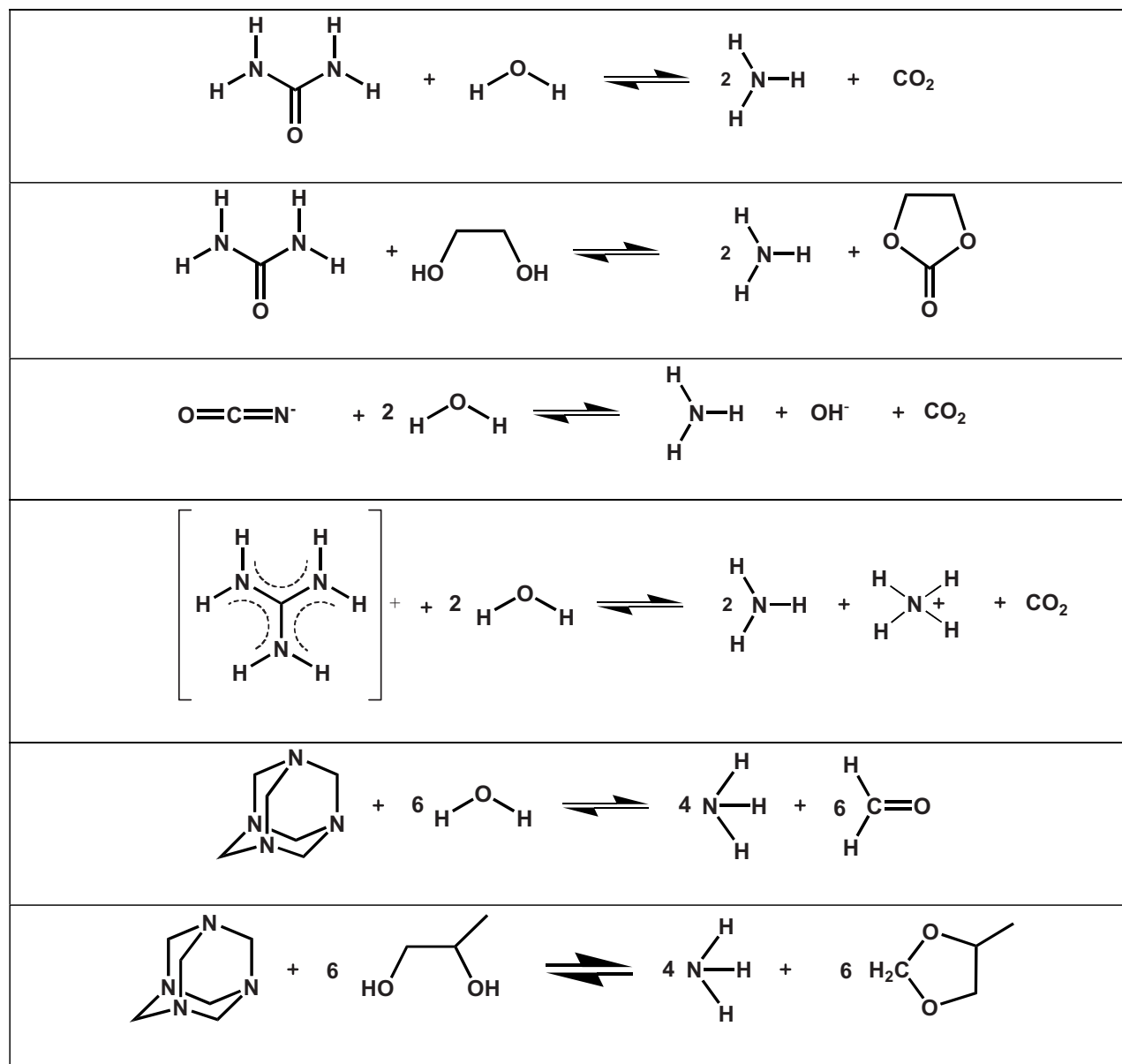
To further explore the feasibility of controlling the size and morphology of the oxides hydrothermally prepared via the use of “latent bases,” we decided to explore formamide (F) and dimethylformamide (DMF) solvents. Besides having higher boiling temperatures ( $210^\circ\text{C}$  for F at  $153^\circ\text{C}$  for DMF) than water, hence enabling a reaction at higher temperatures with lower pressures, such solvents have high solubilizing power due to their higher dielectric constant (110 for F as compared to 75 for water), hence enabling a wider use of precursors.

PTFE vessels, containing  $\text{LiH}_2\text{PO}_4$ , urea, and anhydrous  $\text{FeCl}_2$  dissolved in a formamide/propanediol solution (95-5 by volume), were placed in the autoclave and flushed with  $\text{N}_2$  prior to raising its

temperature to  $150^\circ\text{C}$ . From a survey of various reacting times we deduced that 24 h was the minimum time needed to ensure the nucleation/growth of single-phased  $\text{LiFePO}_4$  powders made of poly-disperse, well-crystallized particles (size: from 50 nm to 2  $\mu\text{m}$ ) having a lozenge shape and lying in the  $ab$  plane with the  $c$ -axis perpendicular to  $ab$  (when  $\text{LiFePO}_4$  is indexed in  $Pnma$ ), as deduced from TEM study (Fig. 3c). In Fig. 3c (left) the particles show a surface effect clearly visible on the high-resolution TEM (HRTEM) image. In fact, the thickness is different from the edge to the center of the particle, which explains the different contrast, but the particle is still  $\text{LiFePO}_4$ .

With the same experimental protocol, reaction time, and temperature, but using DMF rather than formamide, we succeeded in producing  $\text{LiFePO}_4$  powders made of 1–2  $\mu\text{m}$  particles covered with a polymeric layer in Fig. 3d (inset left). Most likely this film is of organic nature, as it was occasionally found to melt under the microscope beam during TEM investigation. This was confirmed by a flash annealing at  $680^\circ\text{C}$  and under Ar atmosphere, which indicated that such a polymeric coating layer does transform into a 3–5 nm carbon layer clearly visible on the HRTEM of Fig. 3d (right). In Fig. 3d, the  $\text{LiFePO}_4$  powders present now 50–200 nm well-crystallized particles having an oblong shape. Such a serendipitous result is of great importance for the use of  $\text{LiFePO}_4$  in Li-ion batteries as it directly provides the carbon nanopainting. Thus, the use of DMF provides an interesting alternative to simplify the synthesis of carbon-coated  $\text{LiFePO}_4$  particles, although we recognize that we do not presently control the nature and composition of the polymer, which most likely results from the interaction between DMF and urea, because it is not observed in the absence of urea. The use of anhydrous  $\text{FeCl}_2$  is proof that water brought by hydrated  $\text{Fe}^{\text{II}}$  sulfate is not needed.  $\text{FeCl}_2$  can be advantageously replaced by inexpensive  $\text{FeCl}_3 + \text{Fe}^\circ$ .

**Table I.** Reaction schemes by which various “latent bases” release a Lewis or Bronsted base (this seems to always be ammonia) via solvolysis reactions in the presence of water or diol-based solvents.



The above reaction based on the use of F could also proceed in the absence of urea, implying that this solvent can act as a “latent base.” Obviously it could not occur via a solvolysis reaction but rather through a temperature-driven decomposition reaction that results in the release of  $\text{NH}_3$  and  $\text{CO}$ , which starts at  $180^\circ\text{C}$  and becomes appreciable near  $200^\circ\text{C}$ , offering another dimension to our concept of latent bases, although it is more difficult to control.

Overall, the aforementioned examples demonstrated the richness of the low-temperature “latent base” synthesis method to produce  $\text{LiFePO}_4$  powders of various morphologies. While each synthesis produced single-phased  $\text{LiFePO}_4$ , we note a spread in the unit cell volumes of about  $3 \text{ \AA}^3$  that we ascribed to the existence of some Li/Fe disorder within the structure based on early neutron diffraction and powder Rietveld refinement studies carried out on hydrothermal or sovothermal-made samples having unit cell volumes of  $293$  and  $289 \text{ \AA}^3$ , respectively. We found such a spread to narrow down to  $0.3 \text{ \AA}^3$  by a postanneal treatment under argon of the low-temperature powders, suggesting that the annealing step tends to

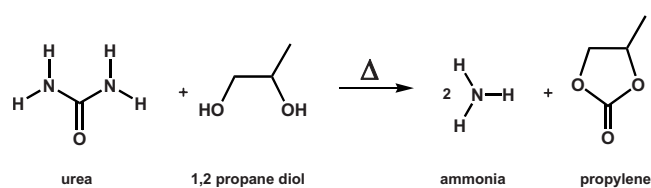
lack the Li and Fe ions in their respective M1 and M2 sites. Although we evidenced the feasibility of manipulating the particle morphology by acting on the base/solvent combinations, we must note that our powders are far from being monodisperse, with size distribution ranging from  $2$  to  $4 \text{ \mu m}$ ,  $200\text{--}800 \text{ nm}$ ,  $50 \text{ nm}$  to  $2 \text{ \mu m}$ , and  $50\text{--}200 \text{ nm}$  when water, water/diol, formamide/diol, and DMF were used as reacting solvents, respectively. Mastering particle coarsening requires tedious field-trial approaches aimed at surveying various synthesis parameters. Further work to improve size uniformity has been undertaken.

Whatever the sample size distribution, Swagelok Li/LiFePO<sub>4</sub> cells were assembled in an argon-filled glove box to check the electrochemical performances on the various batches of LiFePO<sub>4</sub> powders. The cells, using  $1 \text{ M LiPF}_6$  electrolyte solution in  $1:1$  dimethyl carbonate:ethylene carbonate as separator/electrolyte, were cycled at a rate of one lithium in  $10 \text{ h}$ . All LiFePO<sub>4</sub> samples were found to be electrochemically active. However, again for brevity, we solely report data for the most representative samples made in water/diol

**Table II. Summary of the experimental parameters (solvents, latent bases, temperature) used to prepare various LiFePO<sub>4</sub> samples together with the cell parameters of obtained phases. Regardless of the sample,  $\chi^2$  values lower than 3 were obtained for our refinement.**

| Latent base                    | Solvent                                     | Temperature (°C) | Cell parameters (Å)                                       |
|--------------------------------|---|------------------|---|
| Urea                           | Water                                       | 150              | $a = 10.35922(4)$<br>$b = 6.00717(4)$<br>$c = 4.70446(4)$ |
| Urea                           | Water                                       | 160              | $a = 10.34787(5)$<br>$b = 5.99748(4)$<br>$c = 4.69968(4)$ |
| Urea                           | Water                                       | 170              | $a = 10.35727(5)$<br>$b = 6.00254(4)$<br>$c = 4.70532(4)$ |
| Urea                           | Water                                       | 180              | $a = 10.36019(5)$<br>$b = 6.00275(7)$<br>$c = 4.70750(6)$ |
| HMT                            | Water + 2 mL H <sub>2</sub> SO <sub>4</sub> | 150              | $a = 10.35496(5)$<br>$b = 5.99814(7)$<br>$c = 4.70625(4)$ |
| HMT                            | Water + 2 mL H <sub>2</sub> SO <sub>4</sub> | 180              | $a = 10.36791(3)$<br>$b = 6.00658(4)$<br>$c = 4.71104(4)$ |
| Ammonium 2-cyanoéthanoate      | Water                                       | 150              | $a = 10.35697(4)$<br>$b = 6.00286(4)$<br>$c = 4.70709(4)$ |
| Commercial guanidinium sulfate | Water                                       | 150              | $a = 10.35690(3)$<br>$b = 6.00179(4)$<br>$c = 4.70672(4)$ |
| HMT                            | Formamide + 5 mL 1,2-propanediol            | 150              | $a = 10.32599(5)$<br>$b = 5.99040(4)$<br>$c = 4.71266(6)$ |
| Urea                           | DMF + 5 mL 1,2-propanediol                  | 150              | $a = 10.31801(6)$<br>$b = 6.00259(5)$<br>$c = 4.68841(4)$ |
| HMT                            | Absolute ethanol + 5 mL 1,2-propanediol     | 150              | $a = 10.36112(5)$<br>$b = 5.99850(5)$<br>$c = 4.70715(5)$ |
| Urea                           | Water-1,2-propanediol                       | 180              | $a = 10.36042(5)$<br>$b = 6.00853(5)$<br>$c = 4.69908(4)$ |
| Formamide                      | Formamide                                   | 180              | $a = 10.35362(3)$<br>$b = 6.00713(5)$<br>$c = 4.70724(4)$ |

(Fig. 4a) and DMF/diol (as solvolysis agent) (Fig. 4b) solvent mixtures. For the former, the voltage composition curve shows at a C/10



**Scheme 2.**

rate a reversible and sustainable capacity of 150 mAh/g, which is somewhat spectacular knowing that this sample was neither chemically coated nor ever treated at temperatures greater than 200°C. Turning back to the LiFePO<sub>4</sub> powders grown in DMF/diol mixtures, they initially show only weak signs of electrochemical activity, even when hand-milled with 15% C; this is most likely due to the surface polymeric film. To counter such a difficulty, we flash-annealed our powders at 680°C, resulting in 2% carbon coating, as deduced by thermographic analysis (TGA) measurement.<sup>26</sup> Subsequent hand mixing of such coated powders with 15 wt % of additional carbon was shown to give electrodes displaying a sustained reversible capacity of 150 mAh/g at C/10 (Fig. 4b). Such an electrode exhibits

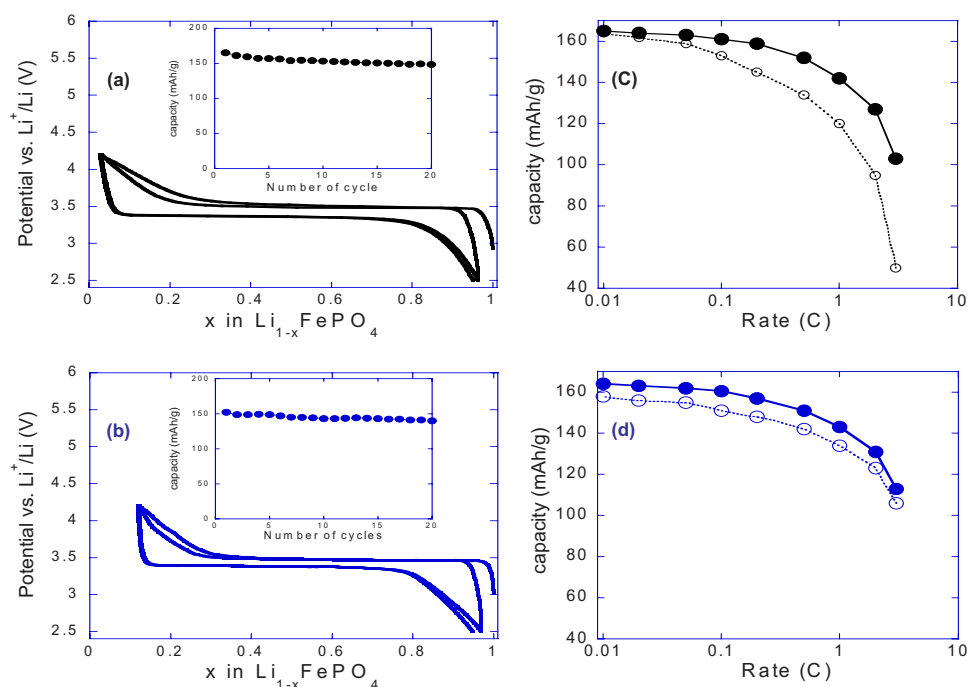


**Figure 4.** (Color online) Room-temperature voltage–composition curves together with capacity retention (inset) are reported in (a) and (b) for samples made out of water/diol and DMF/diol solvent mixtures. The positive electrodes, containing 7 to 10 mg of active material per  $\text{cm}^2$ , were made by ballmilling (Spex 800 for 15 min)  $\text{LiFePO}_4$  powders and carbon SP (carbon black from MM, Belgium) mixtures in a 85–15 wt % ratio. The power rate capabilities of such electrodes, determined using a “signature curve,”<sup>27</sup> are shown in (c) and (d), respectively, with in each case the data for the carbon-free sample (open circles) and carbon-coated sample (full circles). Note that in (d) the open circle data corresponds to a 2% in situ carbon coating (see text) while the full circles data refers to an additional 3% ex situ carbon.

better kinetics than the previous one as evidenced by its lower polarization (50 mV) together with the power rate plot (Fig. 4c). Nevertheless, such rate capabilities are far from today’s state-of-the-art electrodes based on carbon nanopainted  $\text{LiFePO}_4$  powders made from the traditional pyrolysis of sugar precursors at  $700^\circ\text{C}$ . For comparative studies, we applied such treatment to our water-diol-grown  $\text{LiFePO}_4$  powders. The rate capability of such carbon-coated 200–300 nm powders shown in Fig. 4c shows a drastic improvement. Improving further the kinetics of such an electrode will constitute the next stage of our research after the choice of a solvent/temperature/latent base trio for optimal grain size and tap density.

In summary, we have presented an alternative low-temperature synthesis approach for the preparation of  $\text{LiFePO}_4$ . The choice of latent bases is very large, as the possibility of shifting from water to water/glycol of organic solvents alone. Besides acting on the particle size and shape, a side advantage of DMF resides in the growth of a polymer surface layer, which leads to a carbon coating at higher temperatures. Addition of surface active agents during synthesis is also a means of controlling the powder morphology. Although  $\text{LiFePO}_4$  was the main focus, we should mention that this new technique applies to the successful synthesis of a wide variety of electrode materials [ $\text{LiMPO}_4$  ( $M = \text{Mn}, \text{Co}, \text{Ni}$ ),  $\text{Li}_2\text{FeSiO}_4$ ,  $\text{Fe}_2\text{SiO}_4$ ].<sup>25</sup> In short, we believe that such work will open new opportunities to solution chemistry, with the economy of atoms (Li) for sustainability and cost considerations, as the latent bases we used are industrial compounds, and the innocuousness of by-products [e.g.,  $(\text{NH}_4)_2\text{SO}_4$ , a fertilizer], we hope, will lead to industrial processes.

#### Acknowledgments

The authors warmly thank C. Delacourt and C. Masquelier for helpful discussions regarding their experience on solution chemistry, and J-C Jumas for collecting the Mössbauer experiments.

Université de Picardie Jules Verne assisted in meeting the publication costs of this article.

#### References

1. J. M. Tarascon and M. Armand, *Nature (London)*, **414**, 359 (2001).
2. A. K. Padhi, K. S. Nanjundaswamy, and J. B. Goodenough, *J. Electrochem. Soc.*, **144**, 1188 (1997).
3. N. Ravet, J. B. Goodenough, S. Besner, M. Simoneau, P. Hovington, and M. Armand, Abstract 127, The Electrochemical Society Meeting Abstracts, Vol. 99-2, Honolulu, HI, Oct 17–22, 1999.
4. C. Delacourt, P. Poizot, S. Levasseur, and C. Masquelier, *Electrochem. Solid-State Lett.*, **9**, A352 (2006).
5. B. Jin and H.-B. Gu, *Solid State Ionics*, **178**, 1907 (2008).
6. J. Chen, M. J. Vacchio, S. Wand, N. Chernova, P. Y. Zavalij, and M. S. Whittingham, *Solid State Ionics*, **178**, 1676 (2008).
7. C. Xu, J. Lee, and A. S. Teja, *J. Supercrit. Fluids*, **44**, 92 (2008).
8. J. Chen, S. Wang, and M. S. Whittingham, *J. Power Sources*, **174**, 442 (2007).
9. C. Delacourt, P. Poizot, and C. Masquelier, World Pat., WO 20070051 (2007).
10. C. Delacourt, Ph.D. Thesis, LRCS Université de Picardie-Jules Verne, Amiens, France (2005).
11. K. Amine, J. Liu, and I. Belharouak, *Electrochem. Commun.*, **7**, 669 (2005).
12. M. A. Salvado, P. Pertierra, A. I. Bortun, C. Trobajo, and J. R. Garcia, *Inorg. Chem.*, **47**, 7207 (2008).
13. P. Benito, M. Herrero, C. Barriga, F. M. Labajos, and V. Rives, *Inorg. Chem.*, **47**, 5453 (2008).
14. L.-H. Kao, T.-C. Hsu, and H.-Y. Lu, *J. Colloid Interface Sci.*, **316**, 160 (2007).
15. T.-Y. Chen and K.-Z. Fung, *J. Eur. Ceram. Soc.*, **28**, 803 (2008).
16. M. A. Salvado, P. Pertierra, C. Trobajo, and J. R. Garcia, *J. Am. Chem. Soc.*, **129**, 10970 (2007).
17. L. L. Springsteen and E. Matijevic, *Colloid Polym. Sci.*, **267**, 1007 (1989).
18. L. Wang, I. Sondi, and E. Matijevic, *J. Colloid Interface Sci.*, **218**, 545 (1999).
19. I. Sondi and F. Matijevic, *J. Colloid Interface Sci.*, **238**, 208 (2001).
20. J. Rodríguez-Carvajal, Recent Developments of the Program FULLPROF, in *CPD Newsletter 2001*, Vol. 26, p. 12, available at <http://www.iucr.org/iucr-top/news/index.html>. The program and documentation can be obtained from: <http://www.ill.fr/dif/Soft/fp>
21. P. Thompson, D. E. Cox, and J. B. Hastings, *J. Appl. Crystallogr.*, **20**, 79 (1987).
22. C. Delacourt, L. Laffont, R. Bouchet, C. Wurm, J.-B. Leriche, M. Morcrette, J.-M. Tarascon, and C. Masquelier, *J. Electrochem. Soc.*, **152**, A913 (2005).
23. C. Delacourt, C. Wurm, P. Reale, M. Morcrette, and C. Masquelier, *Solid State Ionics*, **173**, 113 (2004).
24. C. Wurm, Ph.D. Thesis, LRCS Université de Picardie-Jules Verne, Amiens, France (2002).
25. C. Yan, L. Zou, D. Xue, J. Xu, and M. Liu, *J. Mater. Sci.*, **43**, 2263 (2008).
26. N. Recham, M. Armand, and J. M. Tarascon, Eur. Pat. 0803233 (2008).
27. M. Doyle, J. Newman, and J. Reimers, *J. Power Sources*, **52**, 211 (1994).